Behaviour model for semi-crystalline polymer, application to crashworthiness simulations

R.Balieu[a,b,c,*], F.Lauro[a,b,c], B.Bennani[a,b,c], B.Bourel[a,b,c], K.Nakaya[d], E.Haran[d]

[a] *Univ Lille Nord de France, F-59000 Lille, France*
[b] *UVHC, LAMIH, F-59313 Valenciennes, France*
[c] *CNRS, FRE 3304, F-59313 Valenciennes, France*
[d] *TOYOTA MOTOR EUROPE, B-1140 Brussels, Belgium*

Abstract

Today polymer materials are frequently used in the transport domain with more severe specification requirements. The behaviour modeling and failure prediction have consequently become a priority. In this paper, an elasto-viscoplastic behaviour model is presented, with non associated plasticity, damage and strain rate effect, which represents the observed behaviours of a semi-crystalline polymer under dynamic loading.

Keywords: Semi-crystalline polymer, Elasto-viscoplastic behaviour model, Non-associated plasticity, Damage, Crashworthiness

1. Introduction

Crashworthiness simulation has been a major factor in enabling automotive manufacturers to achieve a 30 to 50 % reduction in development time and costs over the past decade. Moreover, demand for greater weight savings and occupant protection has required new design concepts and the use of lightweight materials that often have high ductility and a complex failure. The polymer materials in general are good candidates to reach such objectives.
In recent years, there have been more and more polymer behaviour studies

*Corresponding author
Email address: romain.balieu@univ-valenciennes.fr (R.Balieu)

especially in quasi static states. Two approaches are generally used. A phenomenological one, based on the models previously developed for metals to introduced the viscoplasticity (Ho and Krempl, 2002; Colak, 2005) and physical ones where the strain hardening of semi crystalline polymer is interpreted as entropic forces needed to orient the macromolecular chains connected by cross-links (Ayoub et al., 2010; Regrain et al., 2009).
To take the pressure dependence of the polymer matrix into account, some studies have been done by introducing damage models to overcome this problem. The main model used for damage is the Gurson model which describes the growth of spherical cavities under hydrostatic stress (Zari et al., 2008). This introduction results in very complex models in which material parameters are difficult to identify for automotive application, like the length of the macromolecular chain, the number of rigid links per chain, the initial porosity, etc... . The phenomenological approach is therefore more suitable if the non isochoric deformation is taken into account and if a new technique is used to identify behaviour laws at constant strain rate for a large strain rate range (Lauro et al., 2010; Epee et al., 2011).
In this paper, the behaviour model implemented via an usermat subroutine into the finite element code LS-DYNA®, with softening handled by damage model and regularization technique will be presented. The behaviour model is based on the Drucker Prager yield surface (Drucker and Prager, 1952) which takes into account the hydrostatic pressure. The non-associated plasticity is used with a viscoplastic potential based on the Perzyna model. The model parameters (behaviour laws, damage and rate sensitivity) are deduced from experimental tests.

2. Description of the elasto-plastic model

2.1. Pressure dependent yield surface

As the polymer behaviour depends on the kind of loading, it is also necessary to use a non-symmetric yield surface to represent the behaviour difference in tension, compression and shear loading. The Drucker Prager model is a modification of the von Mises criterion, where an extra term is added to introduce the hydrostatic pressure sensitivity. This model considers that the plasticity occurs when the von Mises equivalent stress and the hydrostatic pressure reaches a critical combination. The behaviour surface defined by the Drucker Prager model is given by

$$f\left(\underset{\sim}{\boldsymbol{\sigma}}, \sigma_t\right) = \sigma_e + \eta p - \xi \sigma_t = 0 \tag{1}$$

where σ_e is the equivalent von Mises stress:

$$\sigma_e = \sqrt{\frac{3}{2}\underset{\sim}{\mathbf{S}} : \underset{\sim}{\mathbf{S}}}, \tag{2}$$

$\underset{\sim}{\mathbf{S}}$ is the deviatoric stress tensor

$$\underset{\sim}{\mathbf{S}} = \underset{\sim}{\boldsymbol{\sigma}} - p\ \underset{\sim}{\mathbf{I}}, \tag{3}$$

$\underset{\sim}{\mathbf{I}}$ is the second order unity tensor and p the hydrostatic pressure given by

$$p = \mathrm{tr}(\underset{\sim}{\boldsymbol{\sigma}}) \tag{4}$$

with $\mathrm{tr}(\cdot)$ is the trace of a second order tensor.
σ_t is the behaviour law in tensile loading, η and ξ are material parameters which characterize hydrostatic pressure dependency. η and ξ are the ratio between the behaviour law in tension and compression (σ_c)

$$\eta = 3\frac{\sigma_t/(\sigma_c - 1)}{\sigma_t/(\sigma_c + 1)}, \quad \xi = 1 + \frac{\eta}{3}. \tag{5}$$

2.2. Non-associated plasticity

In the small-strain elastoplastic theory, the total strain rate tensor $\underset{\sim}{\dot{\boldsymbol{\varepsilon}}}$ is additively decomposed into an elastic component $\underset{\sim}{\dot{\boldsymbol{\varepsilon}}}^{el}$ and plastic component $\underset{\sim}{\dot{\boldsymbol{\varepsilon}}}^{p}$

$$\underset{\sim}{\dot{\boldsymbol{\varepsilon}}} = \underset{\sim}{\dot{\boldsymbol{\varepsilon}}}^{el} + \underset{\sim}{\dot{\boldsymbol{\varepsilon}}}^{p} \tag{6}$$

where the superimposed dot denotes the time derivative.
The plastic deformation of the polymer materials is not an isochoric phenomenon. Indeed, the plastic Poisson ratio ν_p measured experimentally, during a tensile test, shows a decrease in function of the longitudinal strain ε_{yy} (Fig. 1). The non-associated plasticity is then used to represent this volume variation. A plastic potential, g, different to the yield surface is used

$$g\left(\underset{\sim}{\boldsymbol{\sigma}}\right) = \sigma_e + \alpha p. \tag{7}$$

The plastic potential gives the direction $\underset{\sim}{\mathbf{n}}$ of the plastic flow. With a non-associated rate independent plasticity, the plastic strain rate tensor $\underset{\sim}{\dot{\boldsymbol{\varepsilon}}}^{p}$ is given by

$$\underset{\sim}{\dot{\boldsymbol{\varepsilon}}}^{p} = \dot{\lambda}\ \underset{\sim}{\mathbf{n}} \tag{8}$$

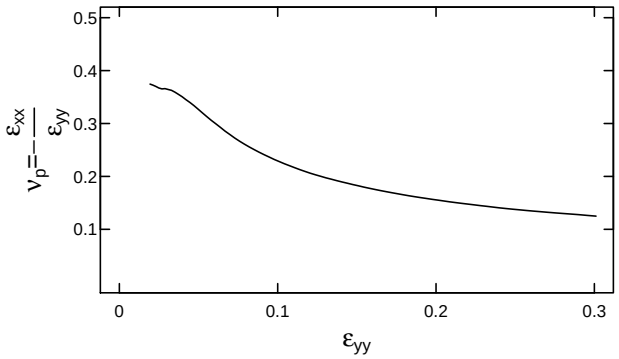

Figure 1: Variation of the plastic Poisson ratio during a tensile test measured on a polypropylene.

where $\dot{\lambda}$ is the rate form of the plastic multiplier λ. The flow direction $\underset{\sim}{\mathbf{n}}$ is performed from the plastic potential by

$$\underset{\sim}{\mathbf{n}} = \frac{\partial g}{\partial \underset{\sim}{\boldsymbol{\sigma}}}. \tag{9}$$

The deviatoric plastic strain rate tensor is given by

$$\underset{\sim}{\dot{\boldsymbol{\varepsilon}}}^p_d = \underset{\sim}{\dot{\boldsymbol{\varepsilon}}}^p - \frac{\underset{\sim}{\dot{\boldsymbol{\varepsilon}}}^p_v}{3}\underset{\sim}{\mathbf{I}} \tag{10}$$

$\underset{\sim}{\dot{\boldsymbol{\varepsilon}}}^p_v$ is the volumetric part of the plastic strain rate tensor

$$\underset{\sim}{\dot{\boldsymbol{\varepsilon}}}^p_v = \mathrm{tr}\left(\underset{\sim}{\dot{\boldsymbol{\varepsilon}}}^p\right). \tag{11}$$

According to equation 8, the deviatoric and the volumetric part of the plastic strain rate tensor is defined as below

$$\underset{\sim}{\dot{\boldsymbol{\varepsilon}}}^p_d = \dot{\lambda}\underset{\sim}{\mathbf{n}}_d, \tag{12}$$

$$\underset{\sim}{\dot{\boldsymbol{\varepsilon}}}^p_v = \dot{\lambda}\underset{\sim}{\mathbf{n}}_v, \tag{13}$$

where $\underset{\sim}{\mathbf{n}}_d$ and $\underset{\sim}{\mathbf{n}}_v$ are the deviatoric and the volumetric part of the flow rule respectively. Assuming the deviatoric and volumetric part of plastic potential, respectively, g_d and g_v, in the current model (Eq. 7), $\underset{\sim}{\dot{\boldsymbol{\varepsilon}}}^p_d$ and $\underset{\sim}{\dot{\boldsymbol{\varepsilon}}}^p_v$ are given by

$$\underset{\sim}{\dot{\boldsymbol{\varepsilon}}}^p_d = \dot{\lambda}\frac{\partial g_d}{\partial \underset{\sim}{\boldsymbol{\sigma}}} = \dot{\lambda}\frac{3}{2}\frac{\underset{\sim}{\mathbf{S}}}{\sigma_e}, \tag{14}$$

$$\dot{\underset{\sim}{\varepsilon}}_v^p = \dot{\lambda}\frac{\partial g_v}{\partial \underset{\sim}{\boldsymbol{\sigma}}} = \dot{\lambda}\frac{\alpha}{3}\underset{\sim}{\mathbf{I}} \tag{15}$$

where α is a material parameter which depends on the plastic Poisson ratio

$$\alpha = \frac{3}{2}\frac{1-2\nu_p}{1+\nu_p}. \tag{16}$$

The parameter α is not a constant value, indeed, the plastic Poisson ratio is in function of the equivalent plastic strain κ as follows

$$\nu_p = y_0 + a\ \exp\left(\frac{\kappa}{t}\right) \tag{17}$$

where y_0, a and t are material parameters determined by experimental tests.

2.3. Damage model

During a tensile test, polymer materials, like polypropylene, have the transversal strains equal to the thickness strains of the specimens. This particular behaviour is called transversal isotropy. Figure 2 shows the true strains measured by Digital Image Correlation (DIC) during a tensile test on a polypropylene. For this measurement, the 2D DIC is used but with two cameras, one for the measurement of the front of the specimens, the other one for the measurement of the thickness of the specimens. Furthermore, the

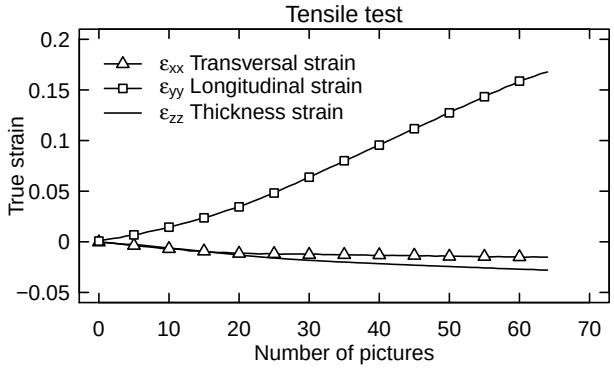

Figure 2: True strains measured by DIC during a tensile test on a polypropylene.

material does not have volume conservation during the plastic deformation and the trace of the strain tensor $\underset{\sim}{\boldsymbol{\varepsilon}}$ is null, like isochoric materials. The

true stress, which takes into account the section reduction, is given by the following relation (by considering $\overrightarrow{y}$ the traction direction)

$$\sigma_{yy} = \frac{F}{S_0} \exp(-\varepsilon_{xx}) \exp(-\varepsilon_{zz}) \tag{18}$$

where S_0 is the initial section. With the transversal isotropy hypothesis, the true stress performed by Eq. 18 becomes

$$\sigma_{yy}^{com} = \frac{F}{S_0} \exp(-2\varepsilon_{xx}). \tag{19}$$

On the other hand, if the true stress is calculated as a incompressible material ($\mathrm{tr}(\underset{\sim}{\boldsymbol{\varepsilon}}) = 0$), Eq. 18 becomes

$$\sigma_{yy}^{inc} = \frac{F}{S_0} \exp(\varepsilon_{yy}). \tag{20}$$

These different hypotheses have a strong impact on the behaviour laws deduced from the experimental tests. Figure 3 shows the effect of the two hypotheses on the true behaviour law performed in tensile loading.

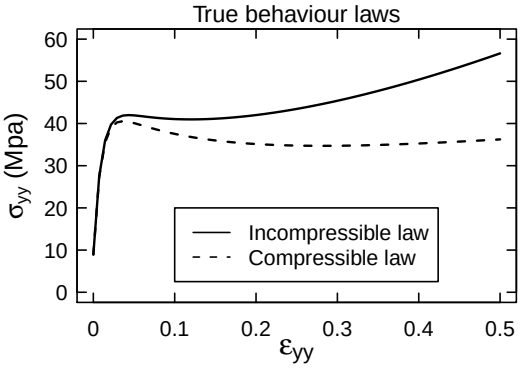

Figure 3: Difference between incompressibility/compressibility hypothesis on the behaviour laws in tension on a polypropylene.

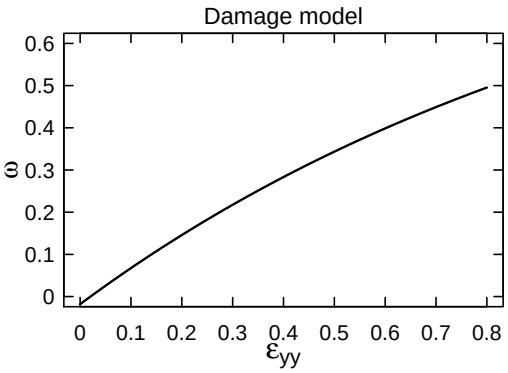

Figure 4: Damage model characterized by tensile tests on polypropylene.

In the current model, the behaviour law used is the incompressible law, which is corrected by a damage model. The damage evolution, D, is also characterized by the ratio between the compressible and the incompressible behaviour law (Fig. 4)

$$D = 1 - \frac{\sigma_{yy}^{com}}{\sigma_{yy}^{inc}}. \tag{21}$$

The damage model used in the numerical model is in function of the equivalent plastic strain κ by

$$D = \begin{cases} 0 & \text{if} \quad \omega(\kappa) \geq 1 \\ 1 - \omega(\kappa) & \text{if} \quad 0 < \omega(\kappa) < 1 \\ 1 & \text{if} \quad \omega(\kappa) \leq 0 \end{cases} \tag{22}$$

where the function $\omega(\kappa)$ takes the following form

$$\omega(\kappa) = b \ \exp\left(\frac{\kappa}{k_c}\right) \tag{23}$$

and b, k_c are material parameters deduced from experimental tests.
By analogy with the classical damage theory, where the effective stress $\underset{\sim}{\boldsymbol{\sigma}}^{\text{eff}}$ is given by

$$\underset{\sim}{\boldsymbol{\sigma}}^{\text{eff}} = \frac{\underset{\sim}{\boldsymbol{\sigma}}}{(1-D)}. \tag{24}$$

The compressible tensile behaviour law in the model is also

$$\sigma_t^{com} = (1-D)\sigma_t^{inc} = \begin{cases} \sigma_t^{inc} & \text{if} \quad \omega(\kappa) \geq 1 \\ \omega(\kappa)\sigma_t^{inc} & \text{if} \quad 0 < \omega(\kappa) < 1 \\ 0 & \text{if} \quad \omega(\kappa) \leq 0 \end{cases} . \tag{25}$$

The yield surface of the model (Eq. 1) becomes

$$f\left(\underset{\sim}{\boldsymbol{\sigma}}, \sigma_t^{inc}, \omega\right) = \sigma_e + \eta p - \xi\omega\sigma_t^{inc} = 0. \tag{26}$$

3. Viscoplastic formulation

As Behaviour law of polymers are highly rate dependent, some experimental tests at different speed loadings are carried out. It is also necessary to take this rate dependency into account on the numerical model. Furthermore, the softening effect introduced by the damaged behaviour law leads to the well known localization problem of deformation in a narrow zone. The finite elements simulation, using the classical continuum plasticity, is not able to describe the softening effect of such ductile materials. This numerical problem leads to a mesh dependency on the response of the finite element model. The localization problem, due to the softening behaviour law in tension, is overcome by using a viscoplastic formulation.

3.1. Perzyna based model

In the small-strain viscoplastic theory, the total strain rate tensor $\underset{\sim}{\dot{\varepsilon}}$ is additively decomposed into an elastic component $\underset{\sim}{\dot{\varepsilon}}^{el}$ and a viscoplastic component $\underset{\sim}{\dot{\varepsilon}}^{vp}$

$$\underset{\sim}{\dot{\varepsilon}} = \underset{\sim}{\dot{\varepsilon}}^{el} + \underset{\sim}{\dot{\varepsilon}}^{vp}. \tag{27}$$

As in classical elasto-plasticity, the viscoplastic strain rate evolves with the flow rule

$$\underset{\sim}{\dot{\varepsilon}}^{vp} = \dot{\lambda}\ \underset{\sim}{\mathbf{n}} \tag{28}$$

where $\underset{\sim}{\mathbf{n}}$ is derived from a plastic potential (Eq. 9) which can be associated or non-associated. In the Perzyna viscoplastic model (Perzyna, 1966) the viscoplastic strain rate tensor is defined by

$$\underset{\sim}{\dot{\varepsilon}}^{vp} = \frac{\left\langle \phi(f^{'}) \right\rangle}{\beta} \underset{\sim}{\mathbf{n}}, \tag{29}$$

with β the viscosity parameter, ϕ the over-stress function that depends on the rate-independent yield surface $f^{'}$. By combining equation 28 with equation 29, the rate form of the plastic multiplier is written as

$$\dot{\lambda} = \frac{\left\langle \phi(f^{'}) \right\rangle}{\beta} \tag{30}$$

where "$\langle \cdot \rangle$ "are the McCauley brackets, such that

$$\left\langle \phi(f^{'}) \right\rangle = \begin{cases} \phi(f^{'}) & \text{if} \quad \phi(f^{'}) \geq 0, \\ 0 & \text{if} \quad \phi(f^{'}) \leq 0. \end{cases} \tag{31}$$

An expression of the over-stress function widely used is

$$\phi(f^{'}) = \left(\frac{f^{'}}{K} \right)^{m} \tag{32}$$

with K commonly chosen as the initial yield stress and m the calibration parameter. In the current model, the over-stress function has been chosen to deduce the calibration strain rate parameter m directly from experimental results. The rate-dependent tensile behaviour law σ_t^v, determined by experimental tests at different speed loadings, takes the following form

$$\sigma_t^v = \sigma_t \dot{\kappa}^n \tag{33}$$

with n the strain rate parameter deduced experimentally and $\dot{\kappa}$ the equivalent viscoplastic strain rate

$$\dot{\kappa} = \sqrt{\frac{2}{3}\, \underset{\sim}{\dot{\varepsilon}}^{vp} : \underset{\sim}{\dot{\varepsilon}}^{vp}}. \tag{34}$$

By combining the Perzyna formulation of the plastic multiplier (Eq. 30) and assuming the viscous parameter β set to 1, the deviatoric and volumetric part of the viscoplastic strain rate tensor, respectively, $\underset{\sim}{\dot{\varepsilon}}_d^{vp}$ and $\underset{\sim}{\dot{\varepsilon}}_d^{vp}$ are given by

$$\underset{\sim}{\dot{\varepsilon}}_d^{vp} = \left\langle \phi(f^{'}) \right\rangle \frac{3}{2} \frac{\underset{\sim}{\mathbf{S}}}{\sigma_e}, \tag{35}$$

$$\underset{\sim}{\dot{\varepsilon}}_v^{vp} = \left\langle \phi(f^{'}) \right\rangle \frac{\alpha}{3} \underset{\sim}{\mathbf{I}}. \tag{36}$$

By combining equation 34, 40 and 37 the equivalent plastic strain is given by

$$\dot{\kappa} = \sqrt{1 + \frac{2\alpha^2}{9}} \left\langle \phi(f^{'}) \right\rangle. \tag{37}$$

The rate-independent tensile behaviour law σ_t, in the current model is given by

$$\sigma_t = \sigma_i^t + kpl \left(1 - \exp(w\kappa)\right) \left(1 + h_1\kappa + h_2\kappa^{m_2}\right) \tag{38}$$

with σ_i^t the initial yield stress in quasi-static loading, and kpl, w, $_h1$, h_2, and m_2 hardening parameters determined experimentally. By combining the damaged yield surface (Eq. 26) and the rate-dependent hardening formulation, the rate-dependent yield surface becomes[1]

$$f\left(\underset{\sim}{\boldsymbol{\sigma}}, \kappa, \dot{\kappa}\right) = \sigma_e + \eta p - \xi\omega\sigma_t\dot{\kappa}^n = 0. \tag{39}$$

The evolution of the strain rate tensor, which directly uses the strain rate parameter determined experimentally n is obtained by combining equations 29, 30, 32, 37 and 39

$$\underset{\sim}{\dot{\varepsilon}}^{vp} = \frac{1}{\sqrt{1 + \frac{2\alpha^2}{9}}} \left\langle \left(\frac{\sigma_e + \eta p}{\xi\omega\sigma_t} \right)^{1/n} \right\rangle \underset{\sim}{\mathbf{n}}. \tag{40}$$

[1]In the aim of clarity, in all the following equations, the behaviour law (σ_t) is the incompressible (undamaged) behaviour law (σ_t^{inc}).

In this formulation the parameter K is replaced by the damaged rate-independent behaviour law $\omega\sigma_t$ with its pressure dependent parameter ξ (Eq. 5).
This model has been implemented via an usermat subroutine for the explicit finite elements code LS-DYNA®.

4. Numerical results

4.1. Verification of the mesh independency

In this section, a numerical example is presented to highlight the numerical result independency on the mesh. The numerical example is carried out on a square. The geometry of the problem and the loading conditions are illustrated in Figure 5. For symmetry reasons, the analysis is performed on the quarter of the section with appropriate boundary conditions.

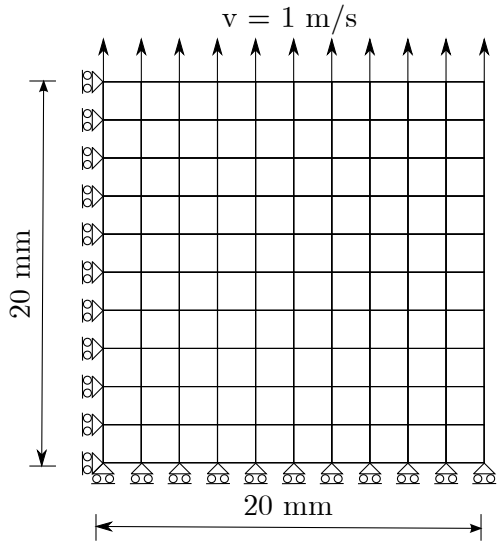

Figure 5: Fine elements mesh.

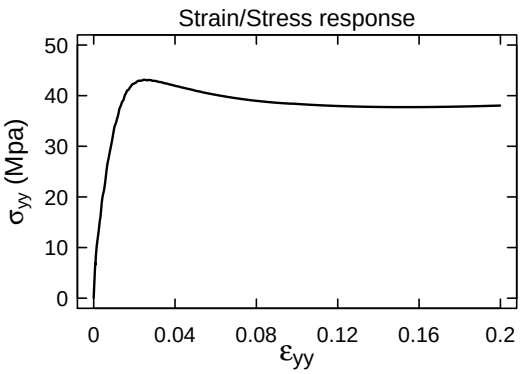

Figure 6: Strain/Stress response on one element.

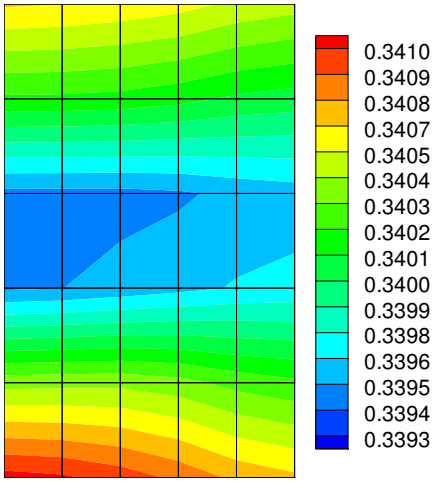

Figure 7: Plastic strain response on the mesh with 25 elements.

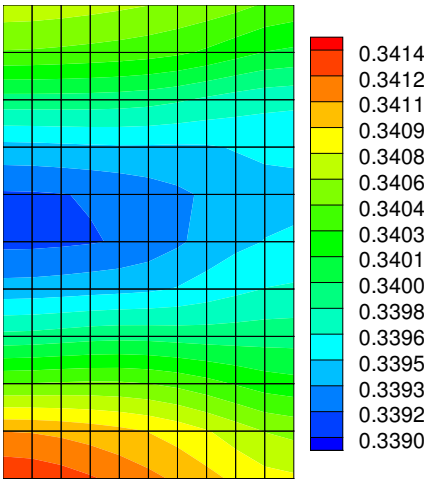

Figure 8: Plastic strain response on the mesh with 100 elements.

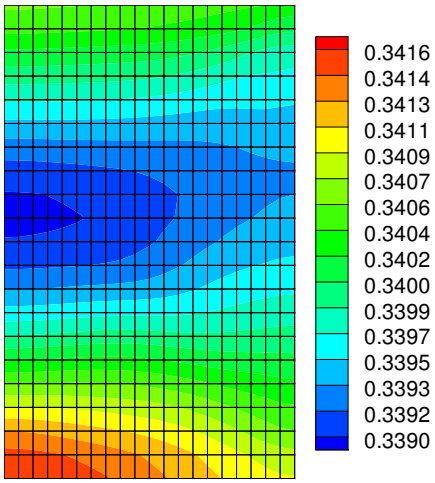

Figure 9: Plastic strain response on the mesh with 400 elements.

Figure 6 shows the behaviour law used for this material (Polypropylene). Three kinds of mesh are used to evaluate the mesh independency on the numerical response. The three models have respectively 25, 100, and 400 elements. All models are meshed with fully integrated shell elements (4 gauss points) and 3 integration points in the thickness. Figure 6 shows the stress response on one element. This stress response shows the softening effect

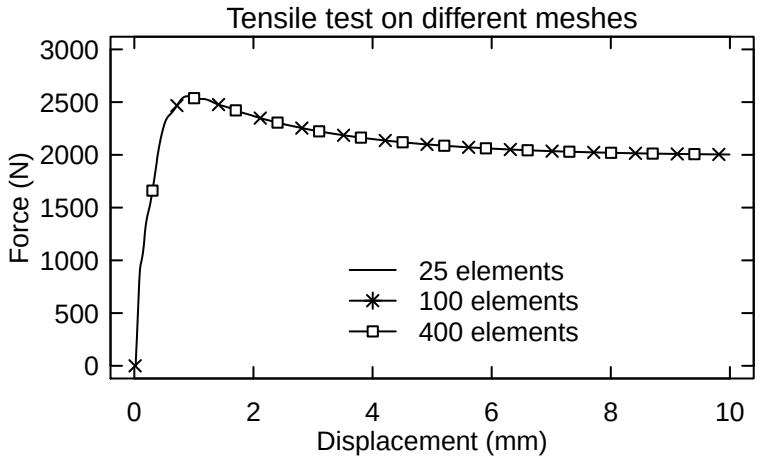

Figure 10: Force response on the tensile test on different meshes.

introduced in the model. The stress response is taken randomly from one element, but Figure 7, Figure 8 and Figure 9 show the same value in terms of plastic strain and also in terms of stress in all the elements for the three models. Figure 10 shows the independency of the mesh on the numerical response.

4.2. Validation of the model on tensile tests

Tensile tests are performed at 3 loading speeds: 0.08 m/s, $0.8m/s$ and $4m/s$. The tests are carried out on normalized tensile specimens. The geometry of the specimens and the loading conditions are illustrated in Figure 11. The specimen is meshed with fully integrated shell elements (4 gauss points) and 3 integration points in the thickness.

As shown in Figure 12, no localization of the strains appears during the tests, the plastic deformation in the length gauge (initially 30 mm) is homogeneous in all the elements. Figure 13 shows a good correlation between the numerical response and the experimental data, in terms of force/displacement for the three dynamic speed loadings. The strain tensor components are shown in Figure 14. ε_{xx} is equal to ε_{zz}, the isotropic transversal behavior is also well modeled.

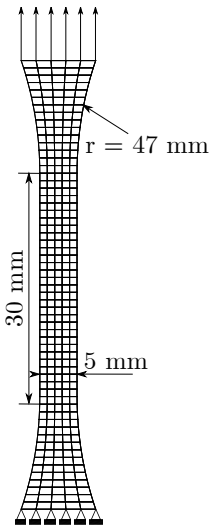

Figure 11: Fine elements mesh.

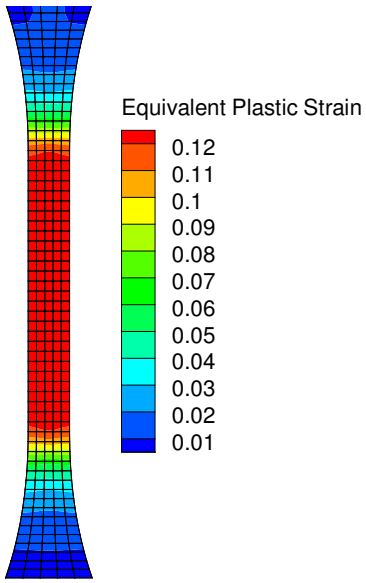

Figure 12: Plastic strain response on the tensile test at 4 m/s.

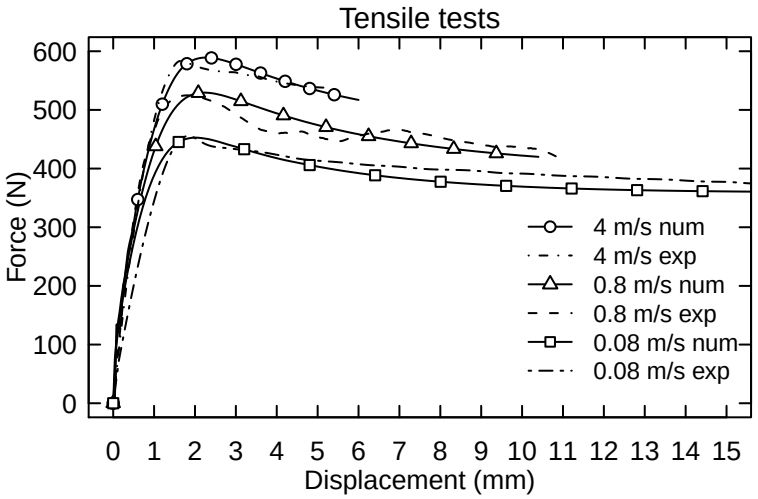

Figure 13: Numerical/Experimental comparison results for 3 loading speeds in tension.

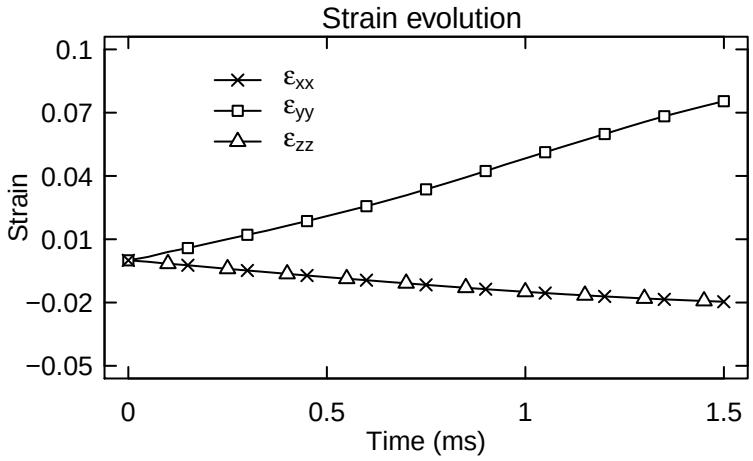

Figure 14: Strain vs time.

5. Conclusion

The implemented elasto-viscoplastic model simulates polymer material such as semi-crystalline polymer. The hydrostatic pressure is modeled by using a non-symmetric yield surface. The plastic potential different to the yield surface takes into account the non-isochoric plastic deformation. The localization problem due to the softening effect introduced by the damaged behaviour law is overcome by a viscoplastic formulation. In the future, a fracture model which takes the hydrostatic pressure and the triaxial stress ratio into account, will be added to the existing model. The complete model will be able to simulate the behaviour of the material until fracture in a structure solicited under dynamic loading.

6. Acknowledgements

The present research work has been supported by Toyota Motor Europe, the International Campus on Safety and Intermodality in Transportation, the Region Nord Pas de Calais, the European Community, the Délégation Régionale à la Recherche et à la Technologie, the Ministère de l'Enseignement Superieur et de la Recherche, and the Centre National de la Recherche Scientifique: the authors gratefully acknowledge the support of these institutions.

References

Ayoub, G., Zari, F., Nat-Abdelaziz, M., Gloaguen, J., 2010. Modelling large deformation behaviour under loading-unloading of semicrystalline polymers: Application to a high density polyethylene. International Journal of Plasticity 26, 329347.

Colak, O.U., 2005. Modeling deformation behavior of polymers with viscoplasticity theory based on overstress. International Journal of Plasticity 21, 145160.

Drucker, D., Prager, W., 1952. Soil mechanics and plastic analysis or limit disign. Quartely of Applied Mathematics 10, 157165.

Epee, A., Lauro, F., Bennani, B., Bourel, B., 2011. Constitutive model for a semi-crystalline polymer under dynamic loading. International Journal of Solids and Structures 48, 15901599.

Ho, K., Krempl, E., 2002. Extension of the viscoplasticity theory based on overstress (vbo) to capture non-standard rate dependence in solids. International Journal of Plasticity 18, 851872.

Lauro, F., Bennani, B., Morin, D., Epee, A., 2010. The see method for determination of behaviour laws for strain rate dependent material: Application to polymer material. International Journal of Impact Engineering 37, 715722. Impact Loading of Lightweight Structures.

Perzyna, P., 1966. Fundamental problems in viscoplasticity. Advances in Applied Mechanics 9, 243377.

Regrain, C., Laiarinandrasana, L., Toillon, S., Sa, K., 2009. Multi-mechanism models for semi-crystalline polymer: Constitutive relations and finite element implementation. International Journal of Plasticity 25, 12531279.

Zari, F., Nat-Abdelaziz, M., Gloaguen, J., Lefebvre, J., 2008. Modelling of the elasto-viscoplastic damage behaviour of glassy polymers. International Journal of Plasticity 24, 945965.